Results of Multiple Attenuation for 2d Curved Interfaces

Lourenildo W. B. Leite, Fábio J. C. Alves, German C. Garabito and Peter H. W. Hubral (UFPa/Brasil)

Abstract

This paper presents results and computational details of the combined CRS-stack and Wiener-Hopf-Levinson prediction (WHLP) operators for multiple attenuation of 2D curved reflectors, here denominated WHLP-CRS method. The deconvolution operation is performed in common-source sections. The used models simulate sections of the Amazon sedimentary basin.

Introduction

The Paleozoic sedimentary basin of the Amazon region are characterized by the presence of diabase sills that vary in number, position, thickness and extension. The sills are considered as important for the process of generation of petroleum (oil and gas) as energy source of heat, and consequently as trap system due to their sealing capabilities. On the other hand, the sills also generate multiples (internal and external) that cause difficulties in the acquisition, processing, interpretation and imaging of reflection time sections. The multiples can dominate and obscure information of the primary reflections, making difficult the interpretation of structures and underlying layers below the sills. This is an undesirable situation for the seismic petroleum exploration of the basin. (Eiras, 1996).

Method

The WHLP-CRS operator for multiple attenuation is the combination of the Wiener-Hopf-Levinson for prediction (WHLP) operator and the common-reflection-surface stack (CRS) operator. The WHLP operator uses the CRS-stack estimations of the wave front attributes (emergence angle β_0 and curvatures K_{NIP} and K_N) to calculate the time-space moving windows. These windows serve to introduce the theoretical periodicity necessary between the primary and its multiple in the WHL operator. The normal equation is modified to:

$$\sum_{k=0}^{N-1} h_k \phi_{gg}(l-k; x_m, h, T_{hyp}) = \phi_{gg}(l+T; x_m, h, T_{hyp}) \, .$$

An important property of the method is that the operator is calculated from the real amplitude of the signal. (Alves et al, 2003).

Results

The performance of the WHLP-CRS operator was evaluated with several synthetic models, and we selected two relevant results to show its efficiency. Figure 1 is a diagrammatic section of the Solimões basin with the presence of diabase sills. Figure 2 is a flat-model with the presence of a high velocity layer, and a common-source time section. Figure 3 is the output of the WHLP-CRS deconvolution operator with the multiple attenuated. The correspondent CRS-stack attributes are shown in Figure 4. Figure 5 presents a curved-model formed by 4 layers over a half-space, and the presence of a high velocity layer to represent a diabase sill. Figure 6 shows the time section of CS 40 (model of Figure 5) without additive noise, before the application of the WHLP-CRS operator, and shows details in zoom of the multiple attenuation. Figure 7 corresponds to CS 40 as Figure 6, but with additive noise, before and after the application of the WHLP-CRS operator, and shows details of the multiple attenuation. We observe that the amplitudes of the primary and of its multiple look close to the amplitude of the additive noise. Even this way, the WHLP-CRS operator attenuates the multiple with efficiency. Figure 8 shows the result of the deconvolution of the windowed segment of the first trace of CS 40 section. Figure 9 are the attribute sections. Figure 10 is a zero-offset section (Figure 5) obtained with the CRS-stack using the wave front attributes of Figure 9.

Conclusions

An important observation is that the concept of time-space shifting windows on the autocorrelation allows the extension of the theory of the WHLP operator, for multiple attenuation in time domain, to configurations where there is no periodicity between primary and its multiple, as is the case of CS and CMP configurations. This makes possible to treat models with dipping-plane and curve interfaces with good and consistent results.

The extension of the conventional WHLP method to admit the CRS-stack is very attractive, what makes the WHLP-CRS a basically data-driven method.

Among the difficulties that we still face are the ones related to conflicts (crossings) between primaries and non related multiples, to the small separations between primaries and their multiples, and to the eternal dipping problem. Another difficulty here, not analyzed in details, has to do with the interpretation of the autocorrelation function.

Acknowledgments

The authors thank the contract PRH-ANP/MME/MCT-UFPa for the financial aid that make possible the development of this research, and to the WIT Consortium of the Geophysics Institute of the University Fridericiana of Karlsruhe, Germany, for its continuous support.

References

Alves, F. J. C.; Leite, L. W. B., Callapino, G. G. and Hubral, P. H. W. Multiple attenuation by the WHLP-CRS method. Submitted to the VIII International Congress of the Brazilian Geophysical Society. Rio de Janeiro. 2003.

Eiras, J. F. Tectonic control on phanerozoic sedimentation of the Solimões basin, northern Brazil. XXXIX Brazilian Geological Congress. Salvador, Brazil.1996.

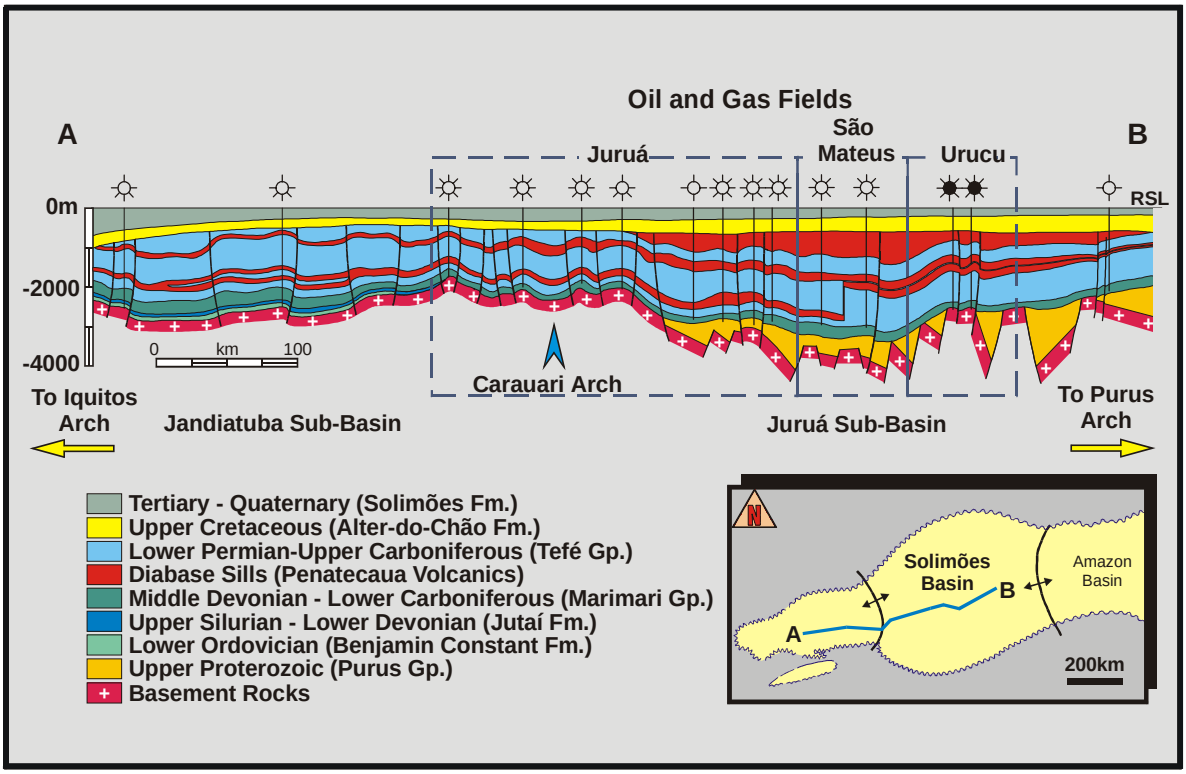

Figure 1. Geological section of Solimões Basin (Amazon region) used for seismic simulations. (Eiras, 1996)

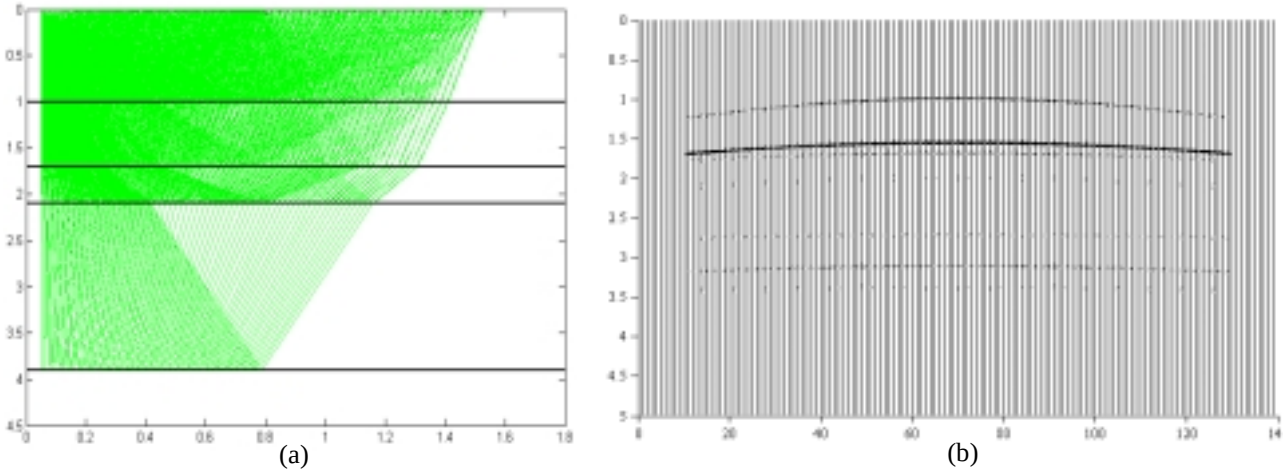

(a) (b)

Figure 2. (a) Example of a Macro-model formed by 4 thick horizontal layers over a half-space, and showing rays. $\Delta x = 12{,}5$ m, $\Delta t = 0.002$ ms, $e_1 = 1.0$ km, $e_2 = 0.7$ km, $e_3 = 0.4$ km, $e_4 = 1.8$ km, $v_1 = 2$ km/s, $v_2 = 2.5$ km/s, $v_3 = 6.0$ km/s, $v_4 = 3.5$ km/s, $v_5 = 5.0$ km/s. (b) Common-shot section, CS.

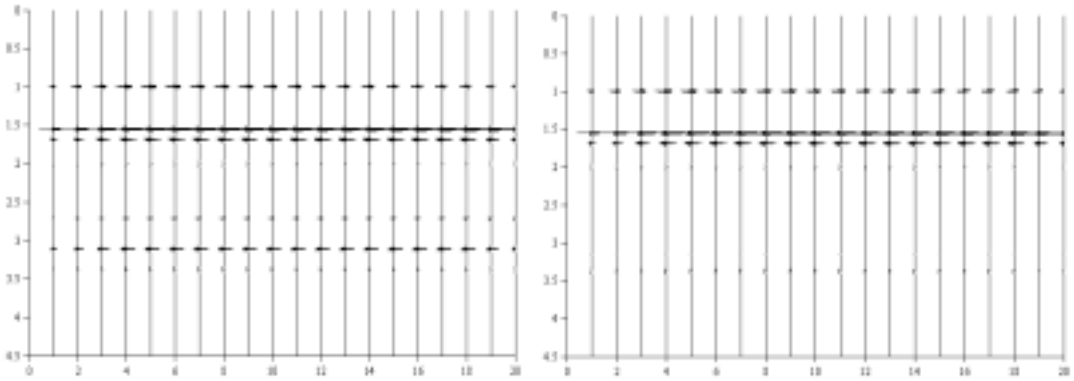

Figure 3. Zero-offset section for comparison. Left: Original section with a multiple present. Right: Output of the WHLP-CRS operator with the multiple attenuated. Model of Figure 2.

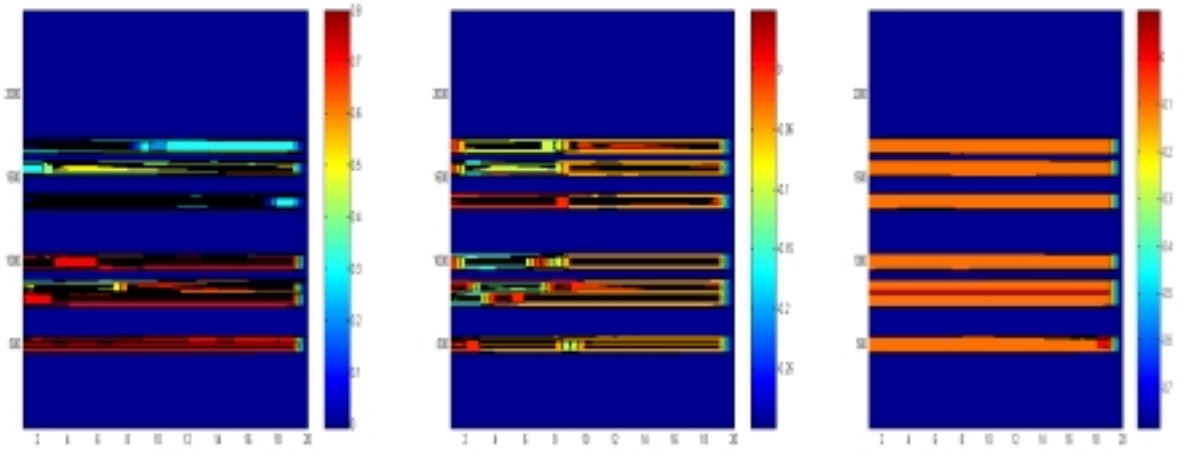

(a) (b) (c)

Figure 4. Attribute sections: (a) K_{nip}; (b) K_n ; (c) Beta. Sections used in the CRS-stack for zero-offset simulation of Figure 2.

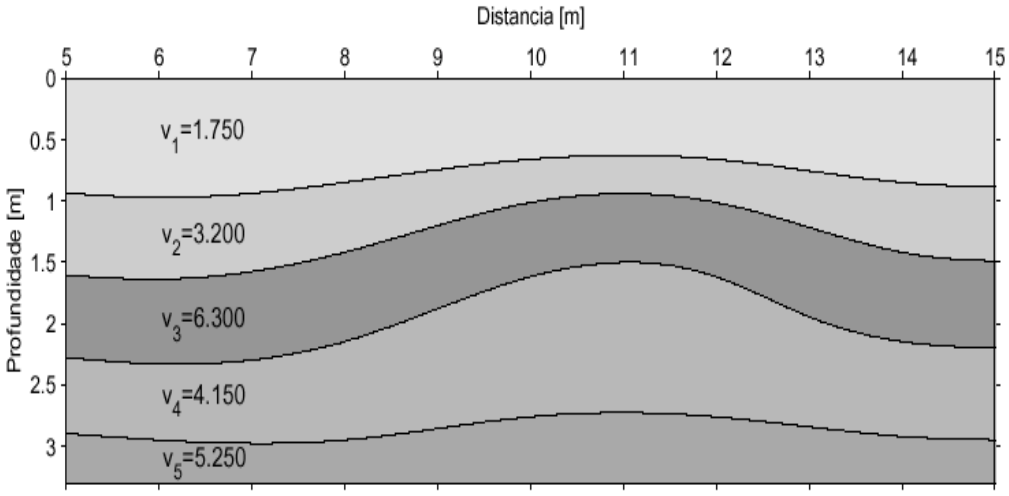

Figure 5. Subsurface model composed of 4 layers over a half-space. The velocities vary from 1750 to 4150 m/s. The high speed layer (6300 m/s) serves to represent a diabase sill. The synthetic data were generated by a ray tracing program. There were computed 201 common-source sections, each with 72 traces, and 50m interval between geophones and shot points. The Gabor function was used to represent the seismic source-pulse with sampling rate of 4 ms. The data contains primary reflections associated with each interface, and a multiple related to the high velocity layer.

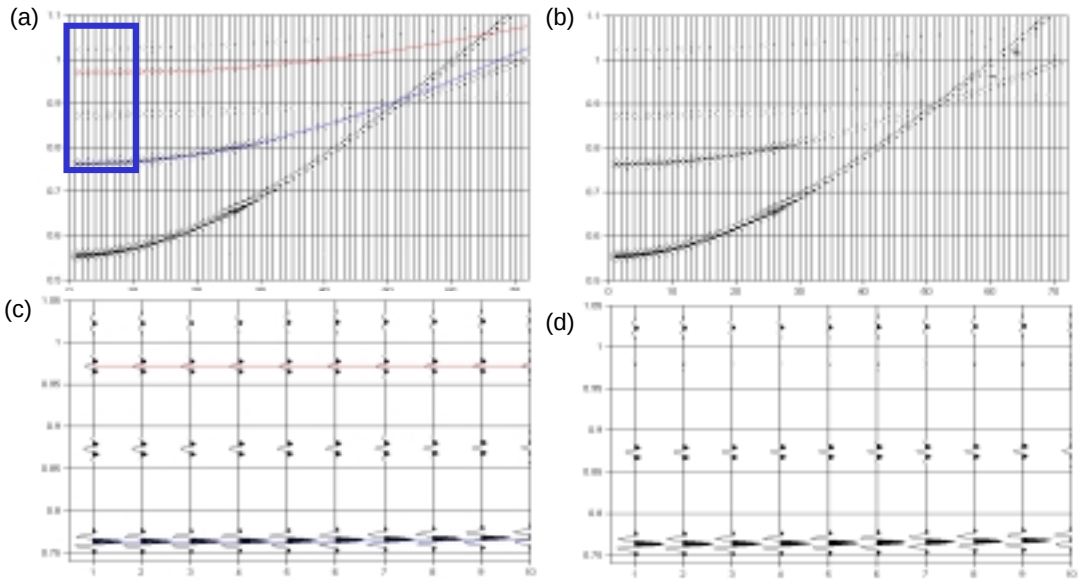

Figure 6. (a) Section CS 40 without additive noise and a multiple present. The blue line indicates the travel time of the primary, and the red line the travel time of the multiple. (b) Section CS 40 with the multiple attenuated. (c) Zoom on the segment indicated by the blue line of item 'a', where the red line indicates a multiple. (b) Zoom on the segment corresponding to the blue line in the section after application of the WHLP-CRS operator with the multiple attenuated.

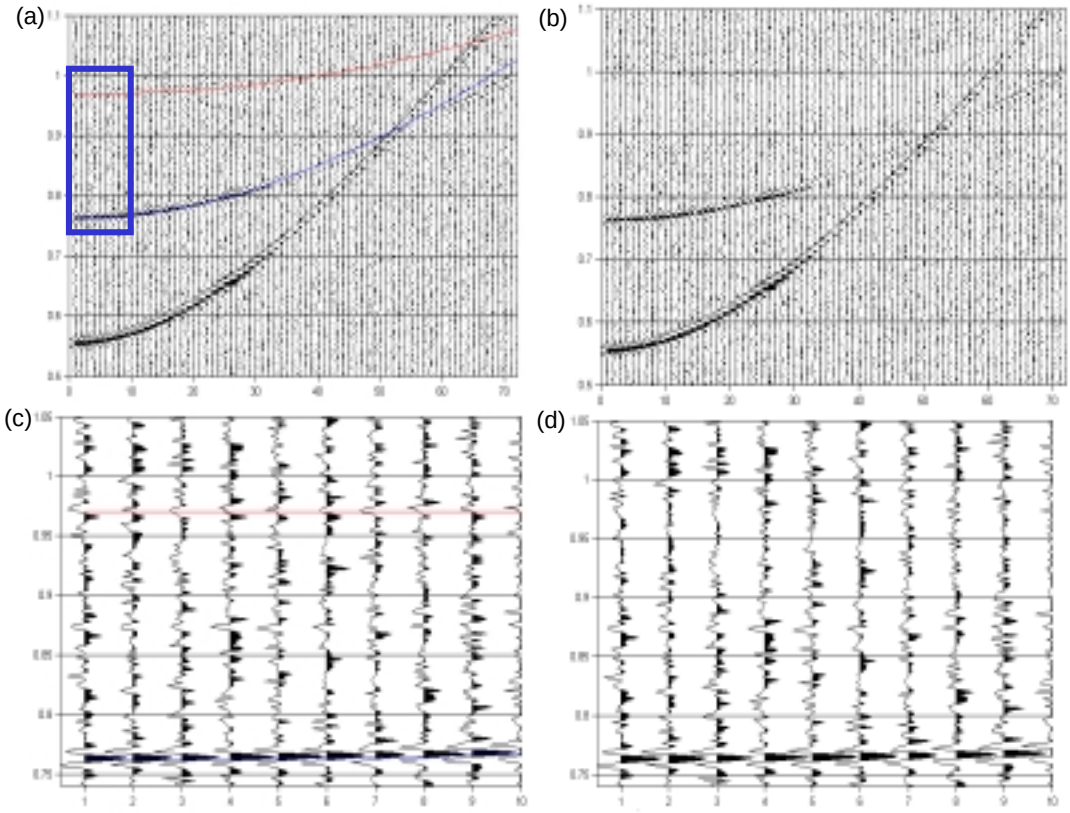

Figure 7. (a) Section CS 40 with additive noise, dynamic gain and the multiple present. The blue line indicates the traveltime of the primary, and the red line indicates the traveltime of the multiple. (b) Section CS 40 with the multiple attenuated. The multiple has a low visualization in this section, but appears clearly in the ZO section, CRS processed. (c) Zoom on the segment marked by the blue line in item 'a', where the red line indicates the multiple. (d) Zoom on the segment corresponding to the blue line in the section after application of the WHLP-CRS operator with the multiple attenuated.

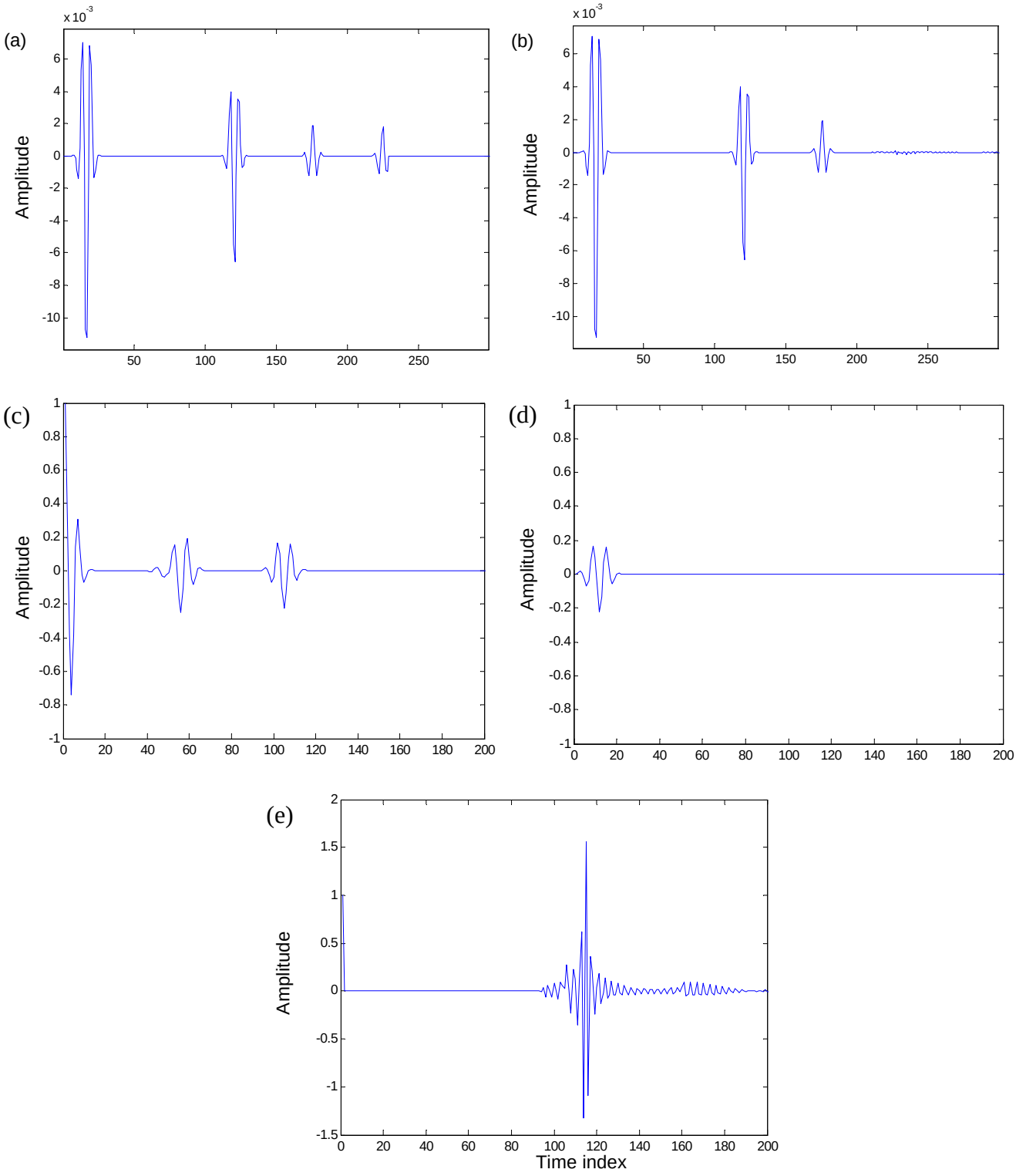

Figure 8. (a) Windowed section of the 1st trace of the CS section (Figure 2). (b) Windowed segment with the multiple attenuated. (c) Autocorrelation of the windowed segment. (d) Crosscorrelation. (e) EPO calculated with the autocorrelation (item 'c') and the crosscorrelation (item 'd') used for multiple attenuation. The performance of the WHLP-CRS operator in multiple attenuation can be seen as good.

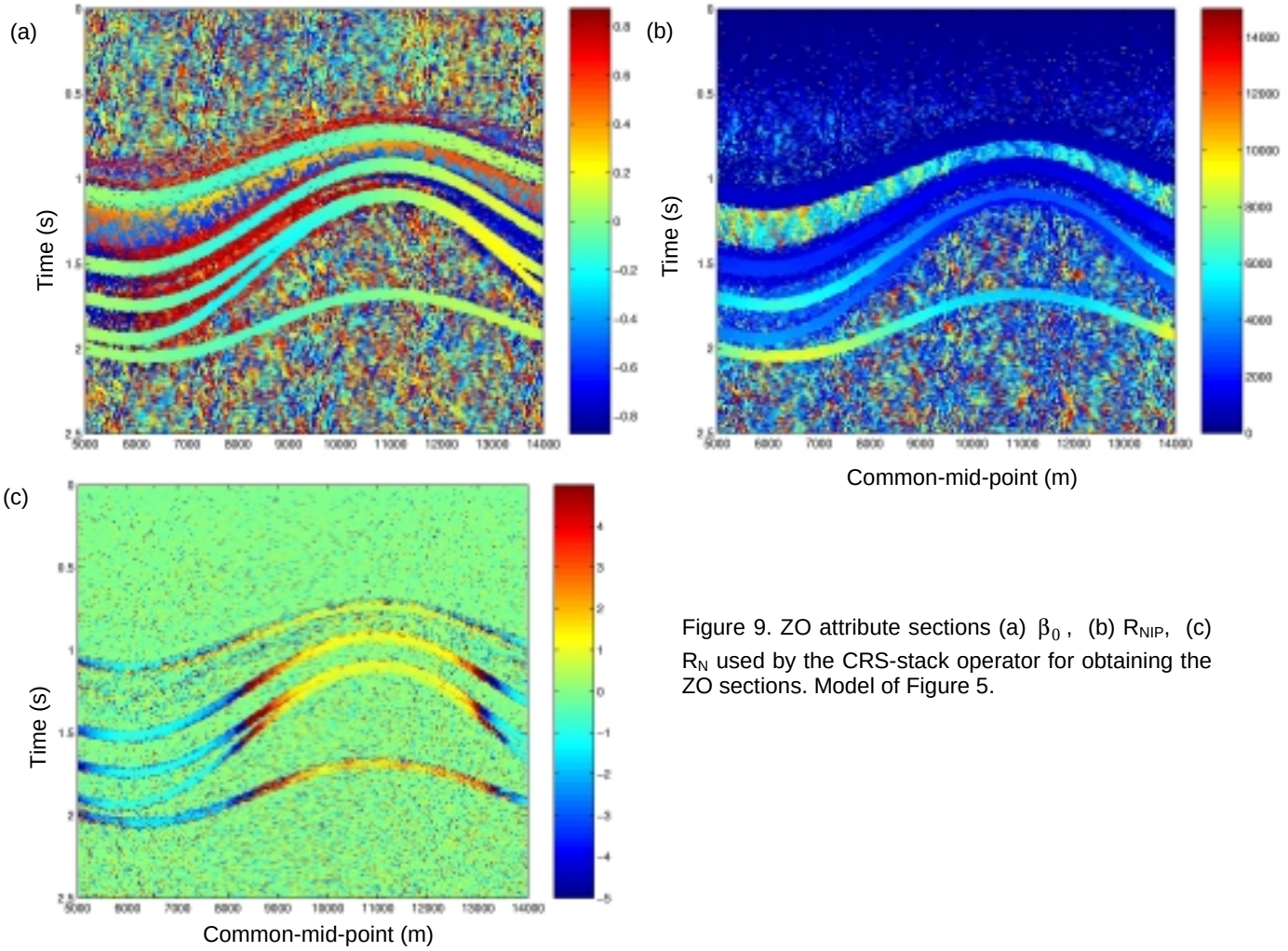

Figure 9. ZO attribute sections (a) β_0, (b) R_{NIP}, (c) R_N used by the CRS-stack operator for obtaining the ZO sections. Model of Figure 5.

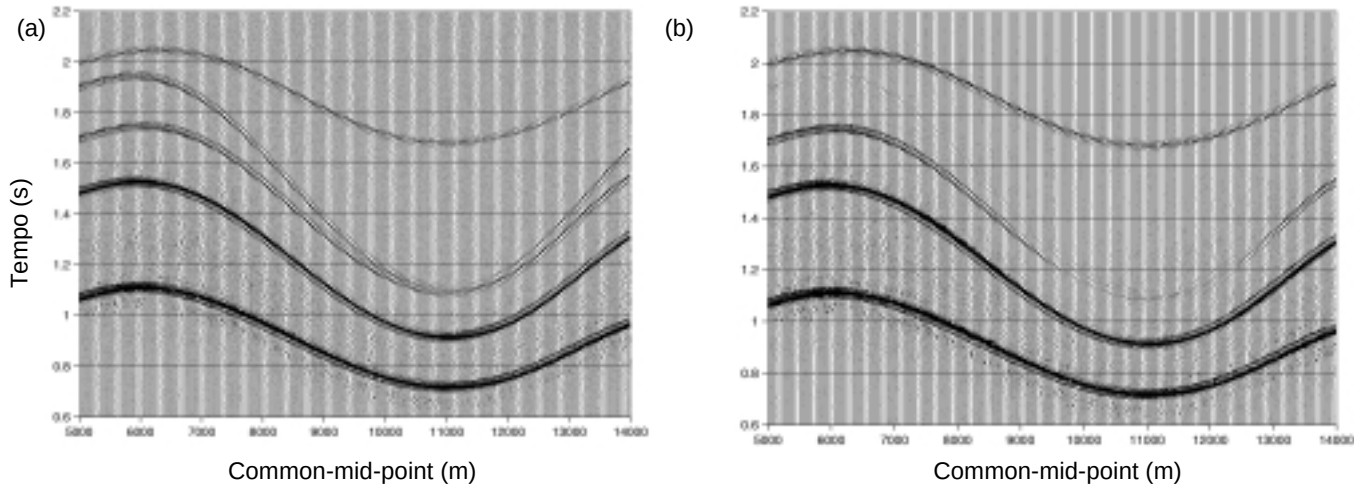

Figure 10. (a) ZO section with dynamic gain resulting from CRS-stack with the multiple present. (b) ZO section with gain resulting from the CRS-stack with the multiple attenuated. We observe a good attenuation, and that the left residue is small as indicated in the ZO section with gain. In the place where the primary and the multiple are very close, the WHLP-CRS operator attenuates both primary and multiple. Model of Figure 5.